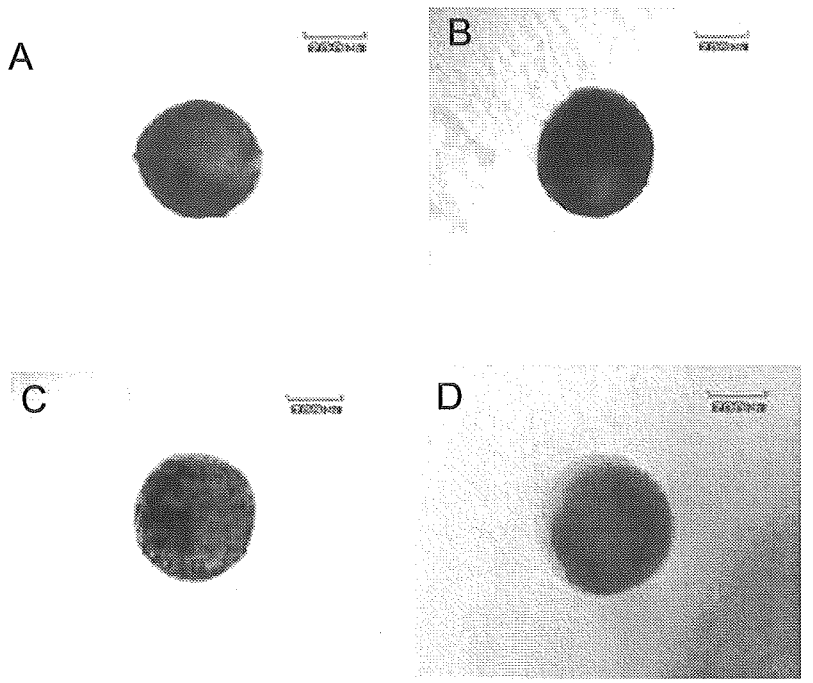

Fig. 5 X-gal staining of Ad vector-transduced EBs.
EBs were transduced with 3000 VP/cell Ad-EF-LacZ (A), Ad-CA-LacZ (B), Ad-RSV-LacZ (C), or Ad-CMV-LacZ (D). Two days after infection, X-gal staining was performed.

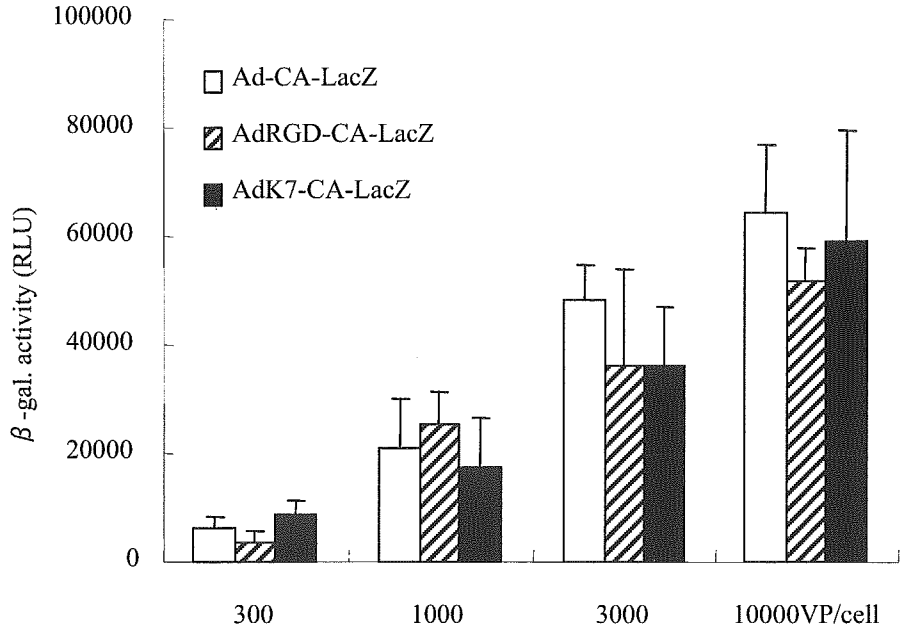

Fig. 6 Dose dependent LacZ expression by fiber-modified Ad vectors in EBs.

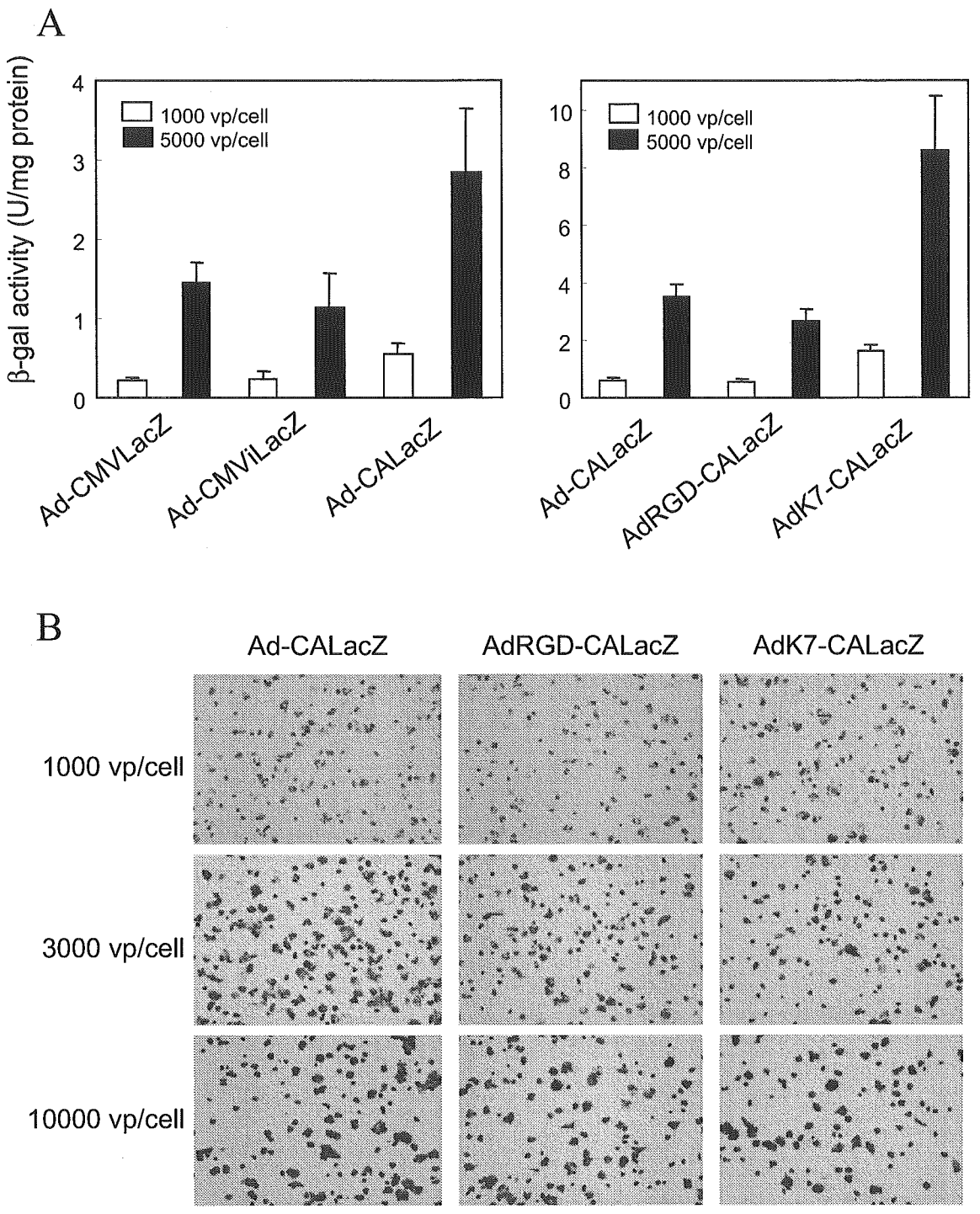

Fig.7 Comparison of the transduction efficiency of various type of Ad vectors into MIN6.
(A) MIN6 were transduced with conventional Ad vectors containing the CMV, CMVi, or CA promoter, and with various types of fiber-modified Ad vectors at 1000 or 5000 vp/cell for one hour. Then, the medium containing the Ad vector was removed and fresh medium was added to the cells. β-galactosidase expression in the cells was measured by a luminescence assay 24 hours later. The data are expressed as mean ± S.D.(n=3). (B) MIN6 were transduced with various types of fiber-modified Ad vectors at 1000, 3000, or 10000 vp/cell for one hour. Then, the medium containing the Ad vector was removed and fresh medium was added to the cells. X-gal staining was performed 24 hours later.

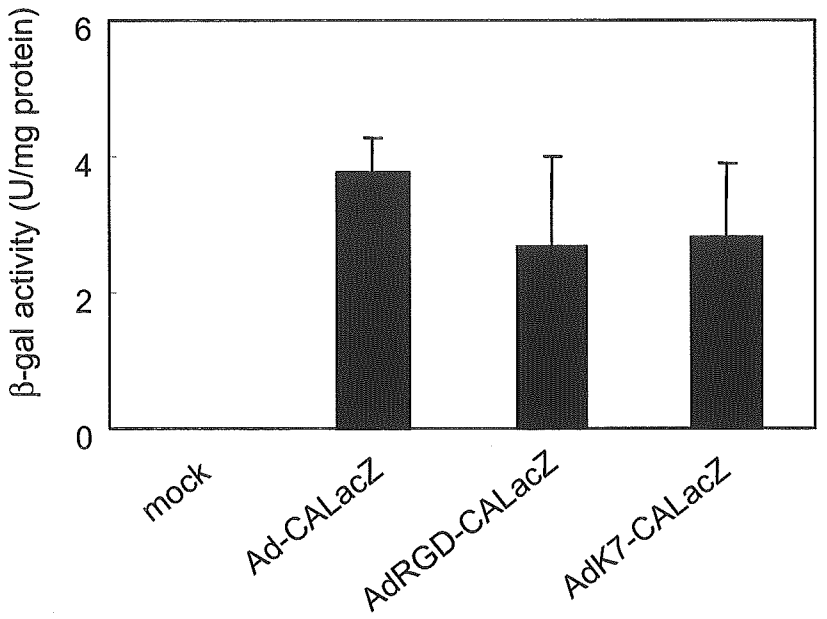

Fig.8 β-galactosidase activity of pancreatic islets transduced with various types of fiber-modified Ad vectors.
Isolated mouse pancreatic islets were transduced with various types of fiber-modified Ad vectors at $2x10^9$ vp/a few hundred islets for one hour. Then, the medium containing the Ad vector was removed and fresh medium was added to the islets. β-galactosidase expression in the islets was measured by a luminescence assay 24 hours later.
The data are expressed as mean ± S.D.(n=3).

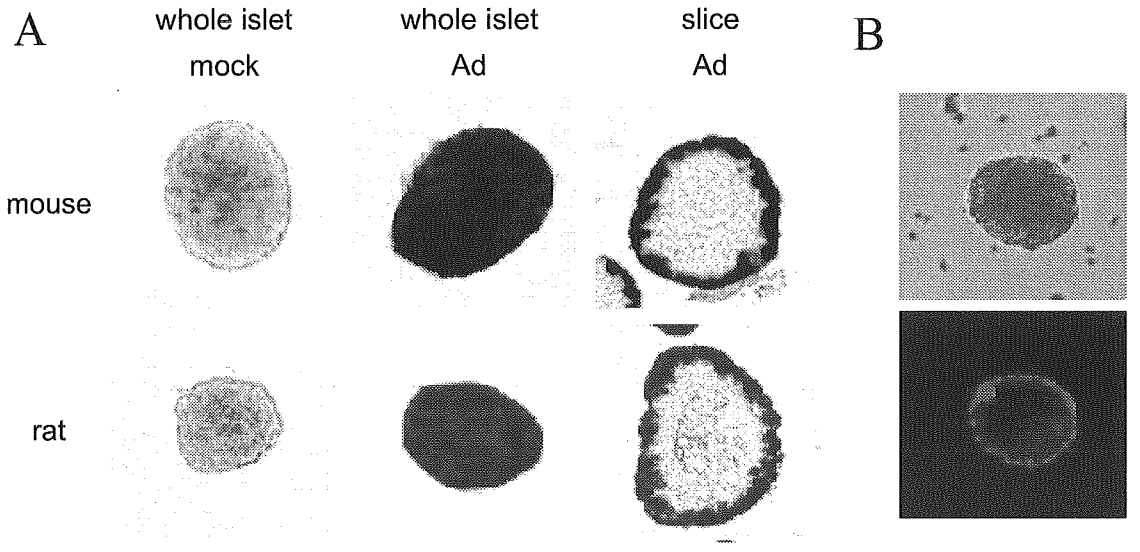

Fig.9 Efficiency of Ad vector transduction into pancreatic islets.
(A) Isolated mouse or rat islets were transduced with $2x10^9$ vp/a few hundred islets of Ad-CALacZ for one hour. Then, the medium containing the Ad vector was removed and fresh medium was added to the islets. X-gal staining was performed 24 hours later. (B) Isolated mouse islets were transduced with $2x10^9$ vp/a few hundred islets of Ad-CAGFP for one hour. Then, the medium containing the Ad vector was removed and fresh medium was added to the islets. Confocal microscopy was performed 24 hours later.

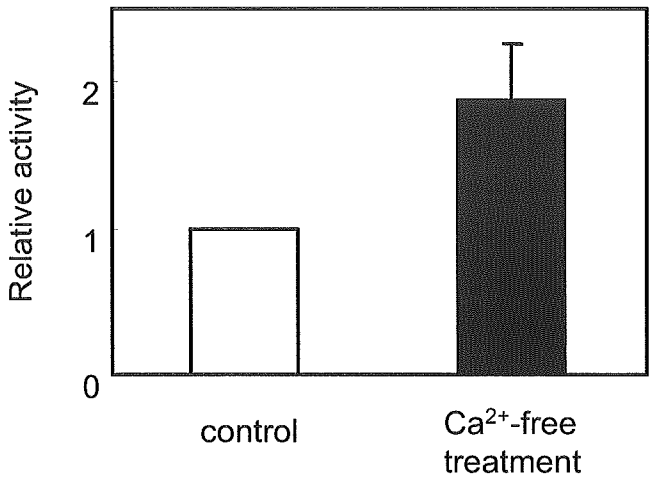

Fig.10 Effect of Ca^{2+}-free treatment on Ad vector transduction into pancreatic islets.
Isolated mouse islets were incubated in Ca^{2+}-free KRB buffer for 15 minutes before they were transduced with $2x10^9$ vp/a few hundred islets of Ad-CALacZ for one hour. Then, the medium containing the Ad vector was removed and fresh medium was added to the islets. β-galactosidase expression in the islets was measured by a luminescence assay 24 hours later. The data are expressed as mean ± S.D.(n=3).

Conventional Ad

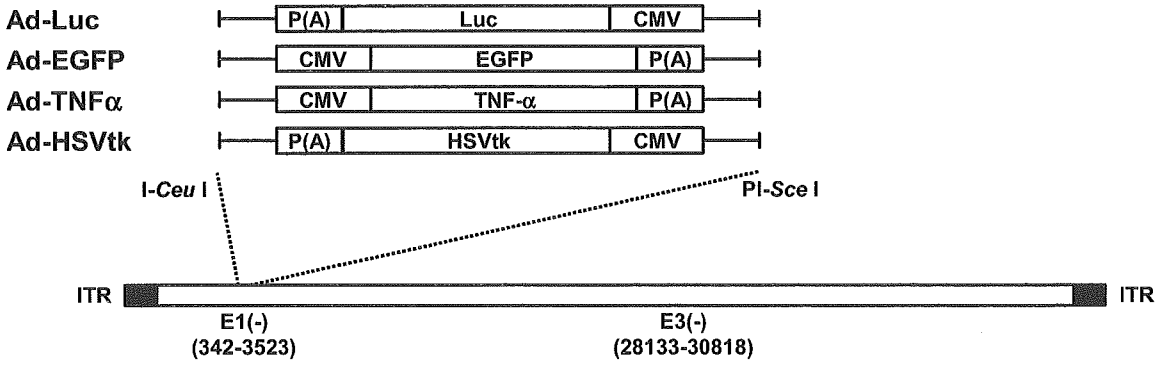

AdRGD

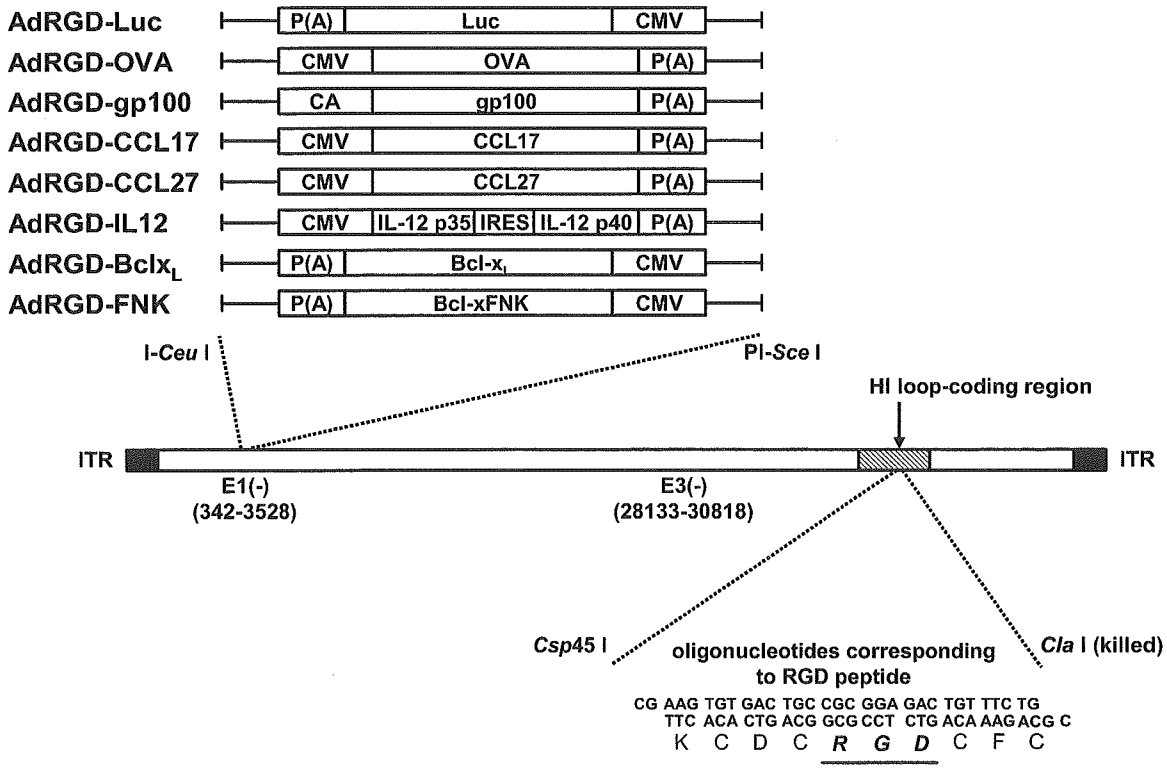

Fig. 11 Schematic representation of conventional Ad and AdRGD used in this study.

Table 2. Primer sequences and reaction parameter used for PCR amplification.

Gene	Primer sequence (5' to 3')	Denaturation	Annealing	Extension	Cycle No.	Product size
Perforin	**(F)** TTTCGCCTGGTACAAAAACC **(R)** CAGTCCTGGTTGGTGACCTT	for 30 s at 95°C	for 30 s at 60°C	for 30 s at 72°C	30	680 bp
Granzyme B	**(F)** CTCGACCCTACATGGCCTTA **(R)** GAAAGGAAGCACGTTTGGTC	for 30 s at 95°C	for 30 s at 62°C	for 30 s at 72°C	30	507 bp
IFN-γ	**(F)** GCTTTGCAGCTCTTCCTCAT **(R)** TGAGCTCATTGAATGCTTGG	for 60 s at 96°C	for 60 s at 50°C	for 60 s at 68°C	30	379 bp
ICAM	**(F)** CTGGCTGTCACAGAACAGGA **(R)** AAAGTAGGTGGGGAGGTGCT	for 60 s at 94°C	for 60 s at 54°C	for 60 s at 68°C	30	559 bp
VCAM	**(F)** CCCAAGGATCCAGAGATTCA **(R)** TAAGGTGAGGGTGGCATTTC	for 60 s at 94°C	for 60 s at 54°C	for 60 s at 68°C	30	489 bp
β-actin	**(F)** TGTGATGGTGGGAATGGGTCAG **(R)** TTTGATGTCACGCACGATTTCC	for 30 s at 95°C	for 30 s at 60°C	for 30 s at 72°C	30	514 bp

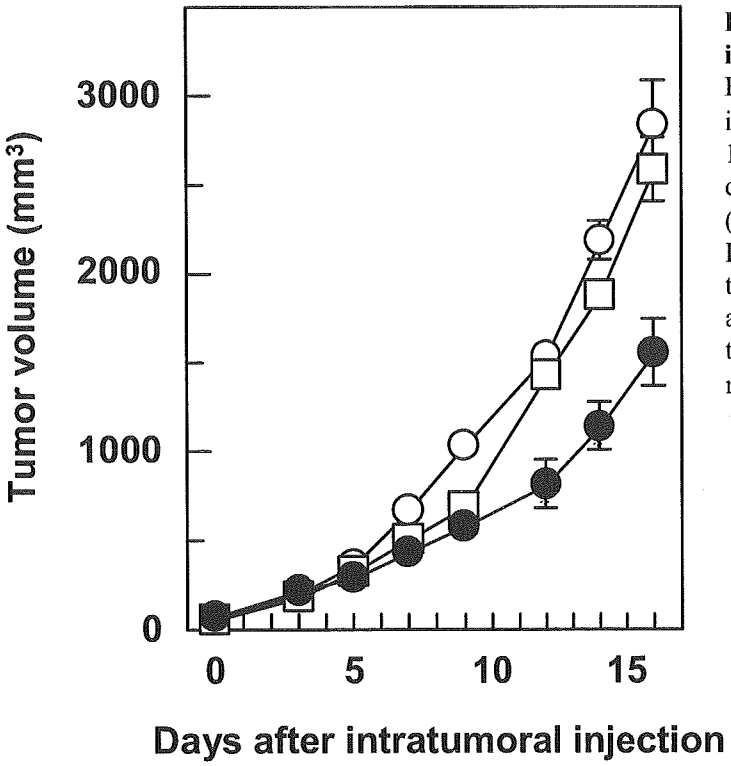

Fig.12 Anti-B16BL6 tumor efficacy of intratumorally injected AdRGD-CCL17. B16BL6 cells were intradermally inoculated into the right flank of C57BL/6 mice at 4 × 10^5 cells/mouse. The tumors (5-7 mm in diameter) were injected with AdRGD-CCL17 (●) or AdRGD-Luc (□) at 3 × 10^8 PFU. Likewise, PBS (○) was injected into the tumors. The tumor volume was calculated after measuring the major and minor axes of the tumor at indicated points. Each point represents the mean ± SE from 6-10 mice.

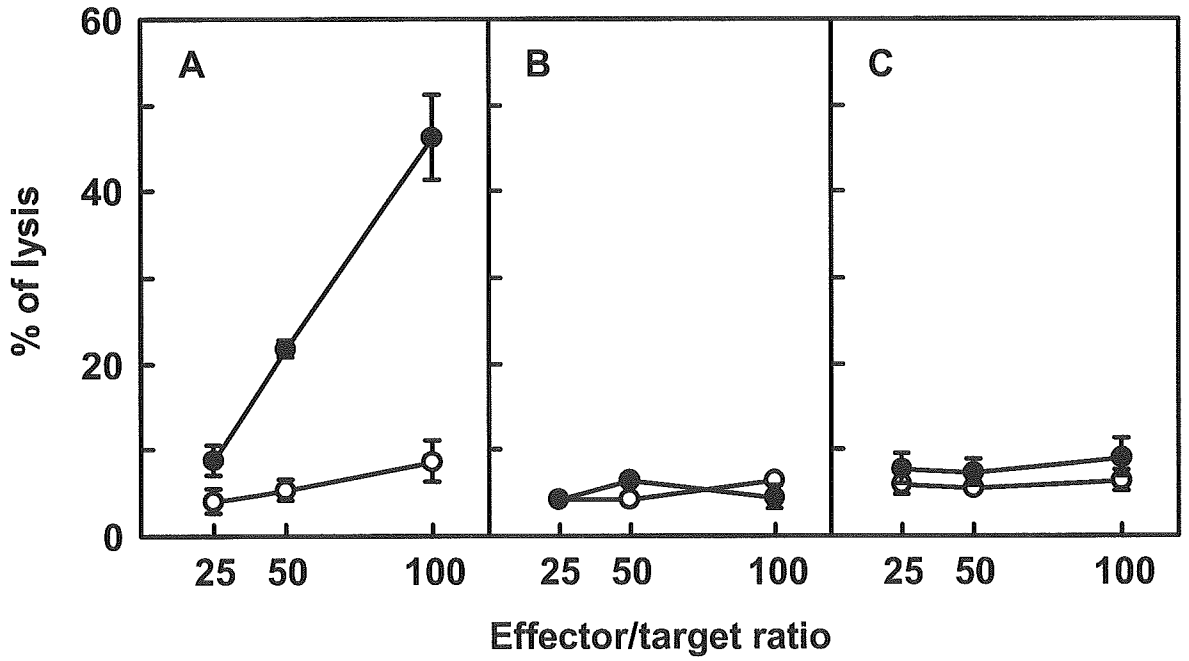

Fig.13 Enhanced tumor-specific CTL activity in B16BL6 tumor-bearing mice by gp100/DC-immunization.
B16BL6 cells were intradermally inoculated into the right flank of C57BL/6 mice at 4 × 10^5 cells/mouse. One day later, the mice were intradermally injected with 10^6 gp100/DCs (●) or PBS (○) in the left flank. At 1 week after immunization, non-adherent splenocytes were prepared from these mice, and then were re-stimulated *in vitro* for 5 days with IFN-γ-stimulated and mitomycin C-inactivated B16BL6 cells. A cytolytic assay using the re-stimulated splenocytes was performed against IFN-γ-stimulated B16BL6 (A), IFN-γ-stimulated EL4 (B), and YAC-1 (C) cells. The data represent the mean ± SE of three independent cultures from three individual mice.

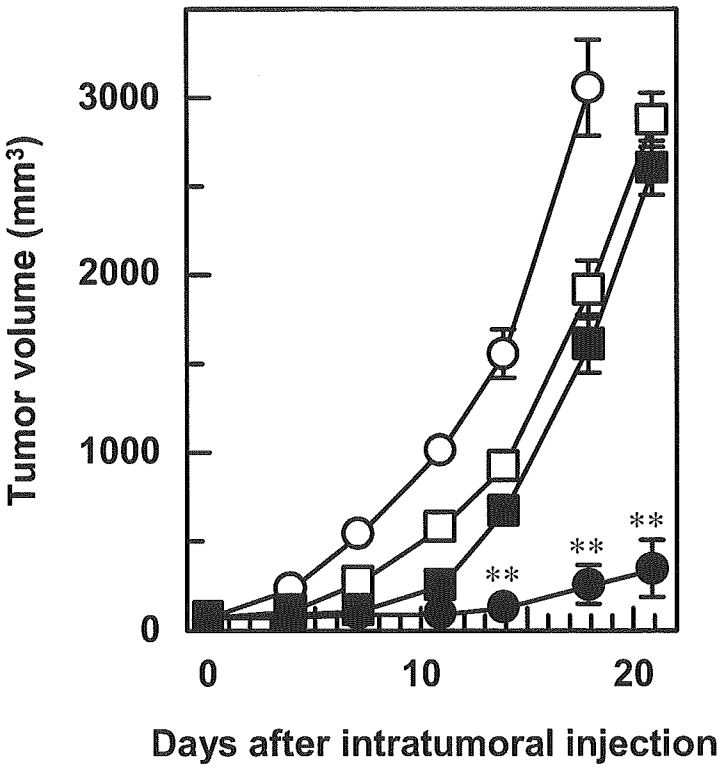

Fig.14 Anti-B16BL6 tumor efficacy of intratumorally injected AdRGD-CCL17 in combination with gp100/DC-immunization.

B16BL6 cells were intradermally inoculated into the right flank of C57BL/6 mice at 4×10^5 cells/mouse. The next day post-tumor inoculation, the mice were intradermally immunized with 10^6 gp100/DCs (●,■,□) or PBS (○) in the left flank. Then, the tumors (5-7 mm in diameter) were injected with AdRGD-CCL17 (●) or AdRGD-Luc (■) at 3×10^8 PFU. Likewise, PBS was administered into control tumors in mice pretreated with gp100/DCs (□) or PBS (○). Tumor volume was calculated after measuring the major and minor axes of the tumor at indicated points. Each point represents the mean ± SE of 7-15 mice. Statistical analysis was carried out by Mann-Whitney *U*-test: *; $p < 0.01$, **; $p < 0.001$ versus AdRGD-Luc-injected group (■).

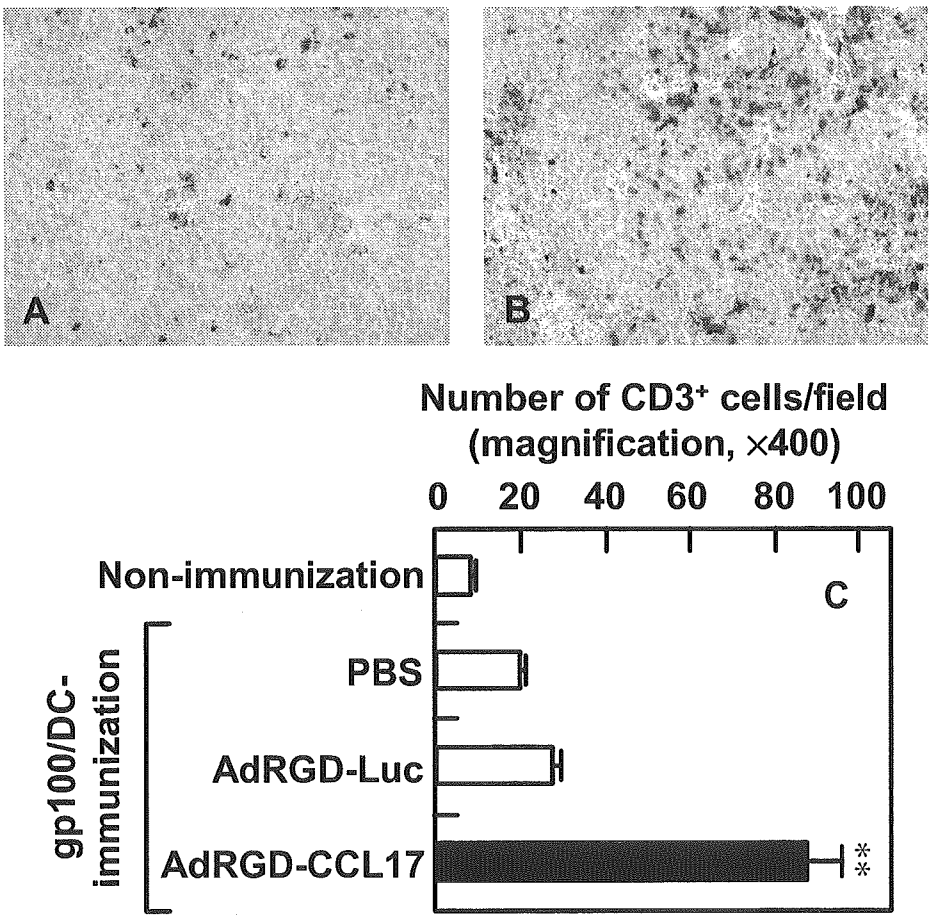

Fig.15 Infiltration of T cells into B16BL6 tumors of mice treated with the combination of gp100/DC-immunization and intratumoral injection of AdRGD-CCL17.

B16BL6 cells were intradermally inoculated into the right flank of C57BL/6 mice at 4×10^5 cells/mouse. The next day, the mice were intradermally injected with 10^6 gp100/DCs in the left flank. Then, the tumors (5-7 mm in diameter) were injected with AdRGD-Luc (A) or AdRGD-CCL17 (B) at 3×10^8 PFU. Likewise, PBS was administered into control tumors. On day 2 after intratumoral injection, immunohistochemical staining against CD3 for determining T cells was performed with frozen tumor sections. A and B; original magnifications are ×200. C; the number of CD3-positive cells in the intratumoral section was assessed by counting six fields per specimen under ×400-magnification. The data represent the mean ± SE of results from three tumors. Statistical analysis was carried out by Welch's *t*-test: **; $p < 0.001$ versus AdRGD-Luc-injected group.

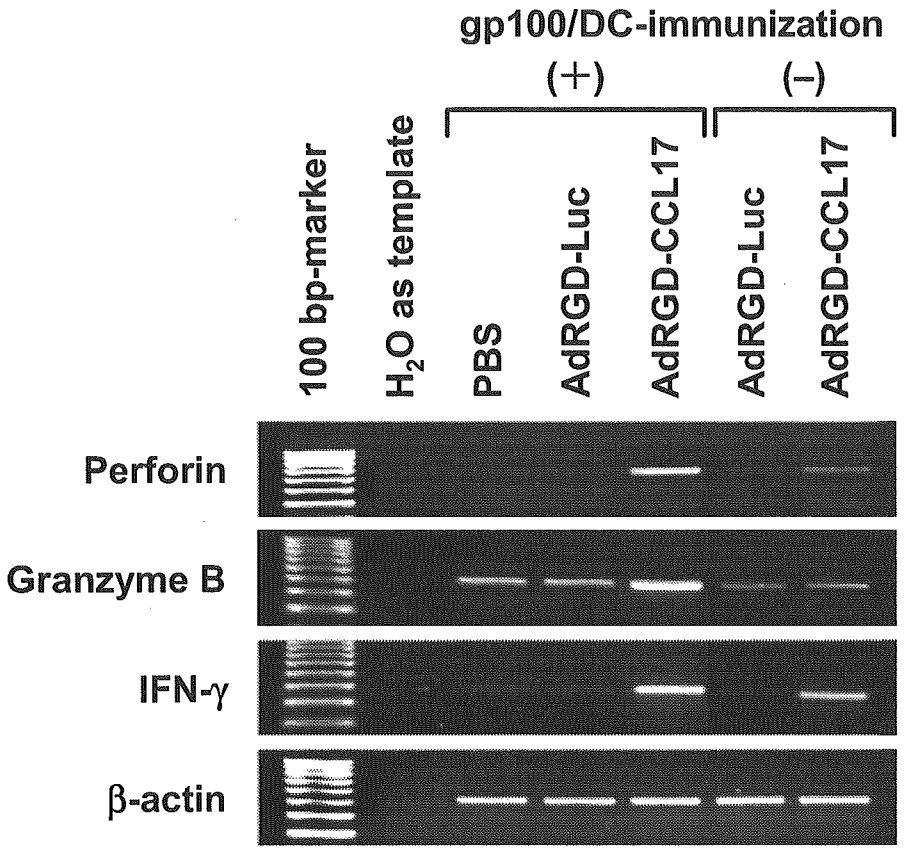

Fig. 16 Activation state of infiltrating immune cells in B16BL6 tumors injected intratumorally with AdRGD-CCL17 in combination with or without gp100/DC-immunization.
B16BL6 cells were intradermally inoculated into the right flank of C57BL/6 mice at 4×10^5 cells/mouse. One day later, the mice were intradermally injected with or without 10^6 gp100/DCs in the left flank. The tumor (5-7 mm in diameter) was injected with AdRGD-CCL17 or AdRGD-Luc at 3×10^8 PFU. Likewise, PBS was administered into control tumors. Two days later, total RNA was isolated from the tumors collected from these mice, and then RT-PCR, specific for perforin, granzyme B, and IFN-γ transcripts, was performed. The PCR products were electrophoresed through a 3% agarose gel, stained with ethidium bromide, and visualized under ultraviolet light.

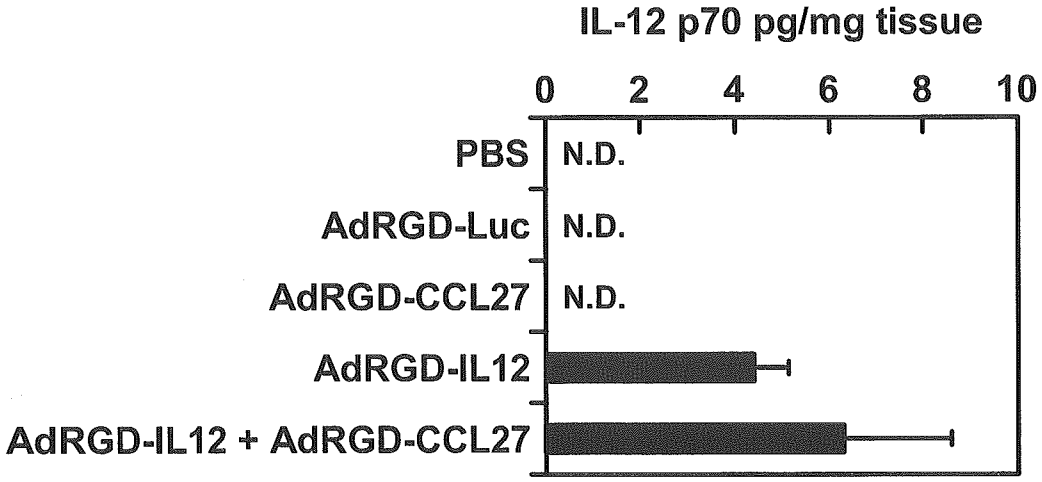

Fig.17 IL-12 production levels in Meth-A tumors injected with AdRGD-IL12 alone or combined with AdRGD-CCL27.

BALB/c mice were intradermally inoculated with 2×10^6 Meth-A cells into the flank. The tumors (9-10 mm in diameter) were injected with AdRGD-Luc alone, AdRGD-CCL27 alone, AdRGD-IL12 alone, or AdRGD-IL12 plus AdRGD-CCL27 in a ratio of 9:1 at the same dose totaling 2×10^7 PFU. PBS was injected into the tumors as a control. Two days later, the tumors were harvested, and then IL-12p70 levels in their homogenates were measured by ELISA. The data represent the mean ± SD of results from three tumors. N.D.: not detectable.

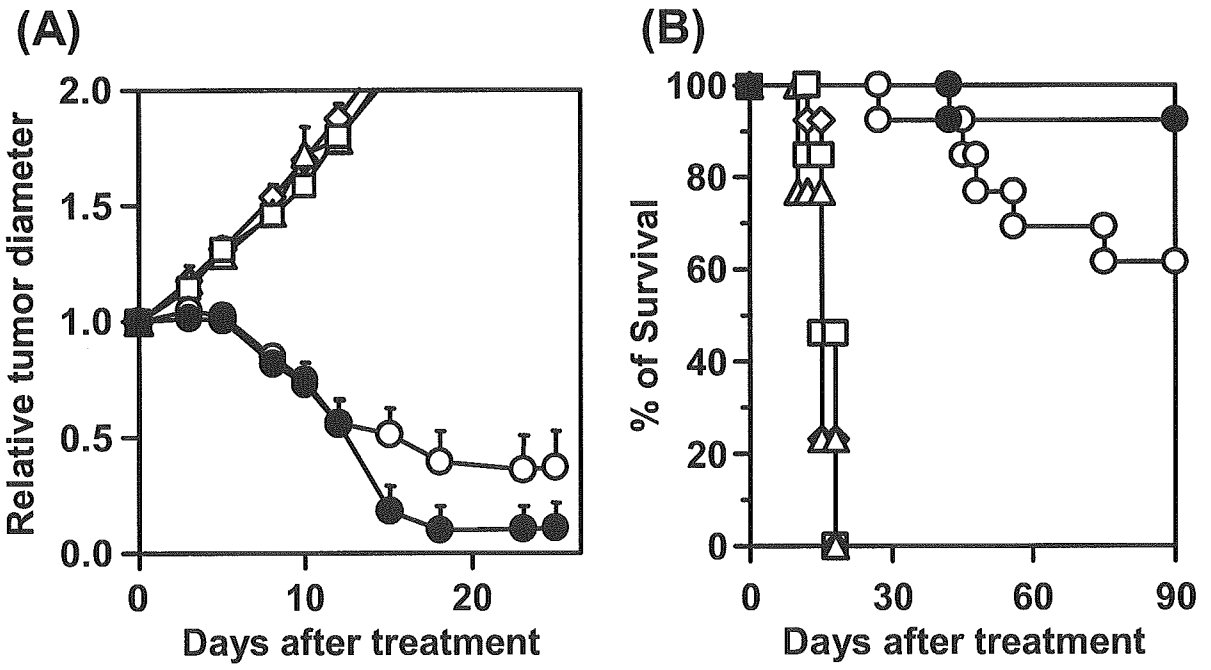

Fig.18 Antitumor efficacy of intratumorally injected AdRGD-IL-12 plus AdRGD-CCL27 in Meth-A tumor model.

BALB/c mice were intradermally inoculated with 2×10^6 Meth-A cells into the flank. The tumors (7-9 mm in diameter) were injected with either AdRGD-Luc alone (△), AdRGD-IL-12 alone (○), AdRGD-CCL27 alone (□), or the combination of AdRGD-IL-12 and AdRGD-CCL27 in a ratio of 9:1 (●) at the same dose totaling 2×10^7 PFU. PBS (◇) was injected into the tumors as a control. (A): The sizes of growing tumors were measured twice a week using microcalipers. Data are expressed as the ratio to the initial tumor diameter. Each point represents the mean ± SE of results from 7 or 8 mice. (B): Data represent the number of mice for which tumors were smaller than 20 mm, expressed as a percentage of the total mice tested in each group.

Table 3. Induction of long-term specific immunity in mice which could achieve complete regression of the primary Meth-A tumor by intratumoral injection with either AdRGD-IL12 alone or the combination of AdRGD-IL12 and AdRGD-CCL27.

Groups	Rechallenging cells[a)]	Tumor-rejected mice/ tested mice
Intact mice	Meth-A	0/10
	CT26	0/5
Meth-A-regressed mice by the injection with AdRGD-IL12	Meth-A	9/9
	CT26	0/6
Meth-A-regressed mice by the injection with AdRGD-IL12 + AdRGD-CCL27	Meth-A	12/12
	CT26	0/5

[a)] Meth-A or CT26 cells were inoculated at 10^6 or 10^5 cells/mouse, respectively.

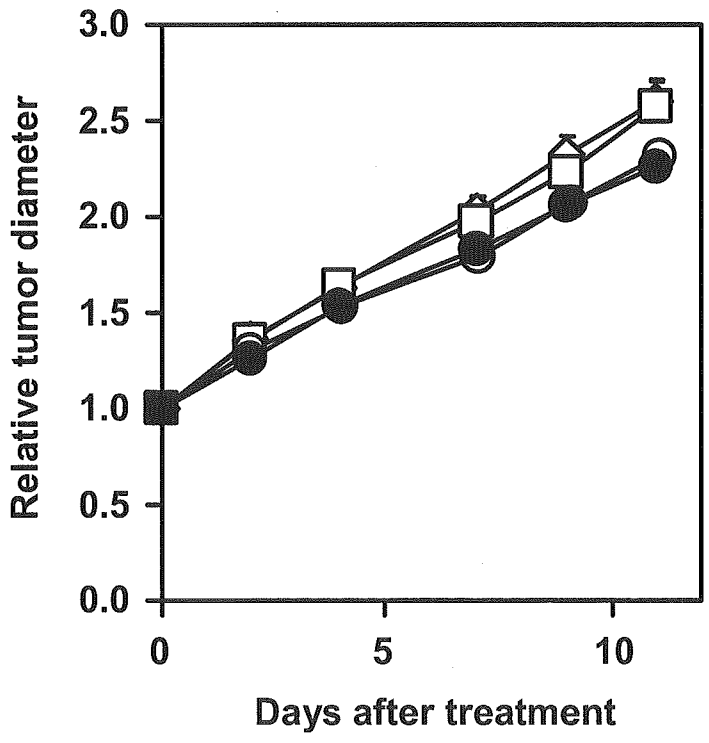

Fig.19 Growth of Meth-A tumors injected with the AdRGD-IL-12 and AdRGD-CCL27 combination in athymic BALB/c nude mice.

BALB/c nude mice were intradermally inoculated with 2×10^6 Meth-A cells into the flanks. The tumors (7-9 mm in diameter) were injected with AdRGD-Luc alone (□), AdRGD-IL12 alone (○), or AdRGD-IL12 plus AdRGD-CCL27 in a ratio of 9:1 (●) at the same dose totaling 2×10^7 PFU. PBS (△) was injected into the tumors as a control. The sizes of growing tumors were measured using microcalipers. Data are expressed as the ratio to the initial tumor diameter. Each point represents the mean ± SE of results from at least six mice.

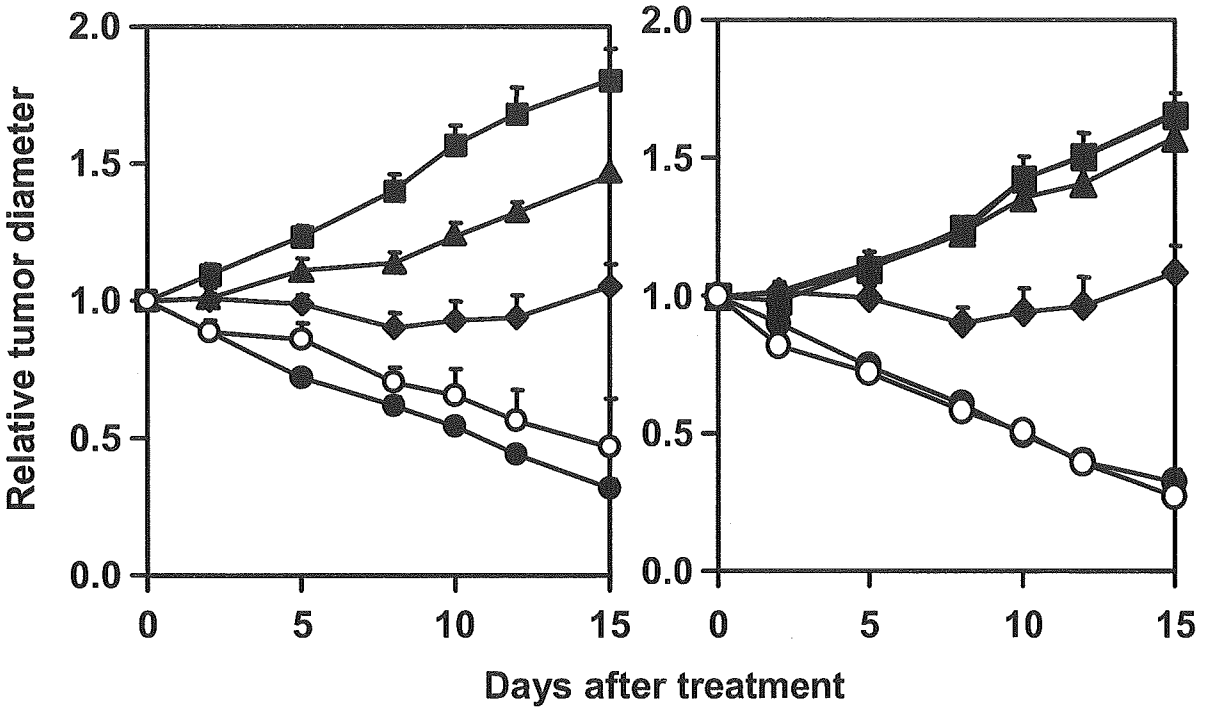

Fig.20 Determination of immune subsets responsible for the antitumor efficacy induced by the IL-12/CCL27 combination.

On day -7, BALB/c mice were intradermally inoculated with 2×10^6 Meth-A cells into the flanks. For depletion of $CD4^+$ T cells (●), $CD8^+$ T cells (▲), or NK cells (◆) in the mice, GK1.5 ascites (anti-CD4), 53-6.72 ascites (anti-CD8), or anti-asialoGM1 antisera were intraperitoneally injected on days -3, -2, -1, 0, 5, 10, and 15. Likewise, for depletion of both $CD4^+$ and $CD8^+$ T cells (■), mice were injected with GK1.5 ascites and 53-6.72 ascites. Normal rat serum (○) was injected into the mice as a control. On day 0, Meth-A tumors received the AdRGD-IL12/AdRGD-CCL27 combination intratumoral injection in a ratio of 9:1 totaling 2×10^7 PFU. Tumor growth was monitored twice a week. Data are expressed as the ratio to the initial tumor diameter. Each point represents the mean ± SE of results from 5-7 mice.

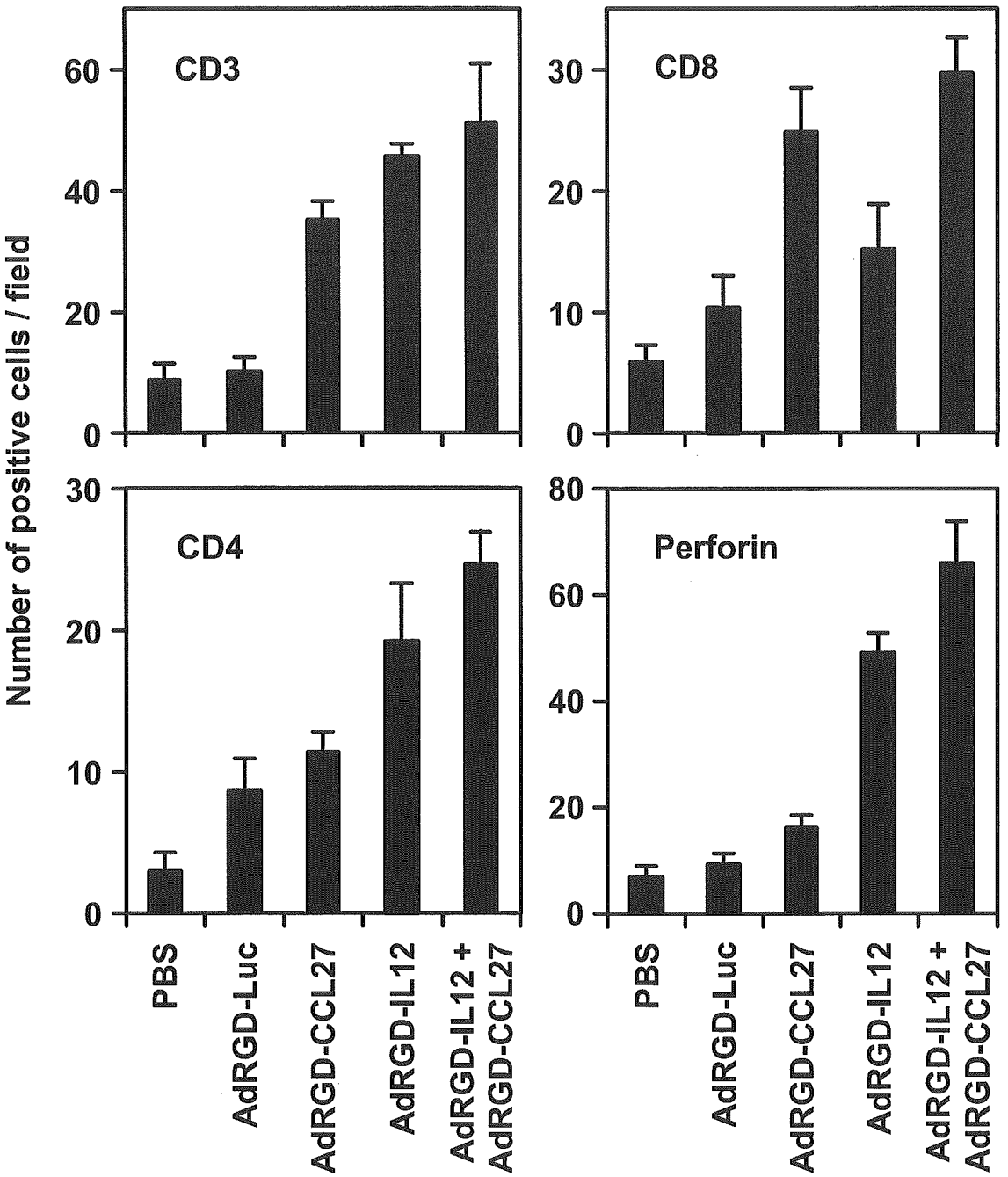

Fig.21 Quantification of tumor-infiltrating T cell subsets and perforin-positive cells in Meth-A tumors injected with the IL-12/CCL27 combination.

Meth-A cells were intradermally inoculated into the flanks of BALB/c mice at 2×10^6 cells/mouse. The tumors (7-9 mm in diameter) were injected with AdRGD-Luc alone, AdRGD-CCL27 alone, AdRGD-IL12 alone, or the AdRGD-IL12 and AdRGD-CCL27 combination in a ratio of 9:1 at the same dose totaling 2×10^7 PFU. PBS was injected into the tumors as a control. On day 6 after the intratumoral injections, immunohistochemical staining against CD3, CD4, and CD8 was performed using frozen tumor sections. These immunohistochemical sections were used to assess the numbers of $CD3^+$, $CD4^+$, $CD8^+$, and $perforin^+$ cells infiltrating into tumor parenchyma by counting six fields per specimen under ×400-magnification. The data represent the mean ± SD of results from three tumors.

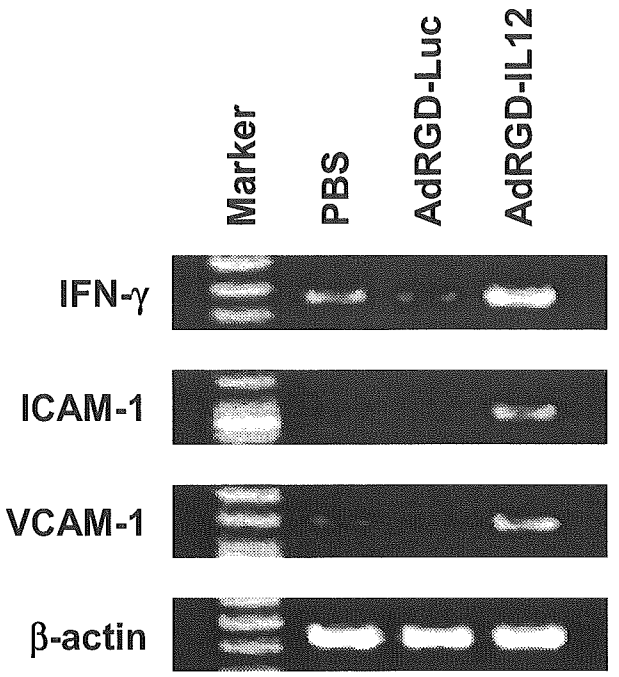

Fig.22 Increases in expression levels of IFN-γ, ICAM-1, and VCAM-1 in Meth-A tumors injected with AdRGD-IL12.
Meth-A cells were intradermally inoculated into the flanks of BALB/c mice at 2×10^6 cells/mouse. The tumors (7-9 mm in diameter) were injected with AdRGD-Luc or AdRGD-IL12 at 2×10^7 PFU. PBS was injected into the tumors as a control. On day 6 after the intratumoral injections, total RNA was isolated from the Meth-A tumors collected from treated mice, and then RT-PCR, specific for IFN-γ, ICAM-1, VCAM-1, and β-actin transcripts, was performed using each primer set descrived in Table 1. The PCR products were electrophoresed through a 2% agarose gel, stained with ethidium bromide, and visualized under ultraviolet light.

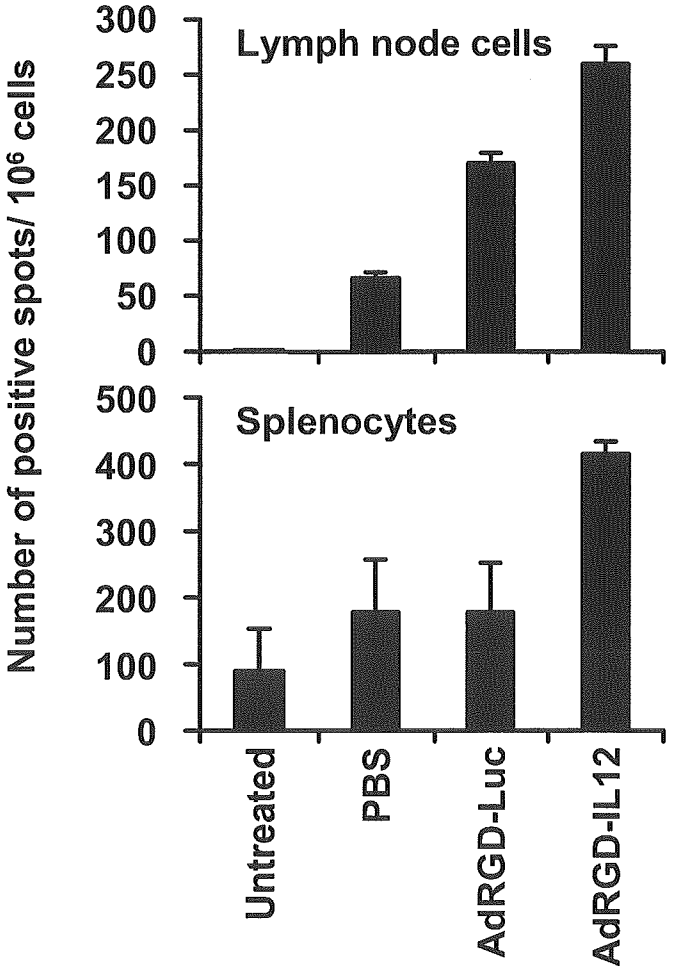

Fig.23 The frequency of IFN-γ producing cells in draining lymph node cells and splenocytes from Meth-A-bearing mice injected with AdRGD-IL12.
BALB/c mice were intradermally inoculated with 2×10^6 Meth-A cells into the flanks. The tumors (7-9 mm in diameter) were injected with AdRGD-Luc or AdRGD-IL12 at 2×10^7 PFU. PBS was injected into the tumors as a control. On day 6 after the intratumoral injections, the draining lymph node cells and splenocytes were prepared from these mice, and then were restimulated *in vitro* with mitomycine C-inactivated Meth-A cells for 24 h. IFN-γ producing cells were evaluated using mouse IFN-γ ELISPOT assay. The data represent the mean ± SE of the results from three mice.

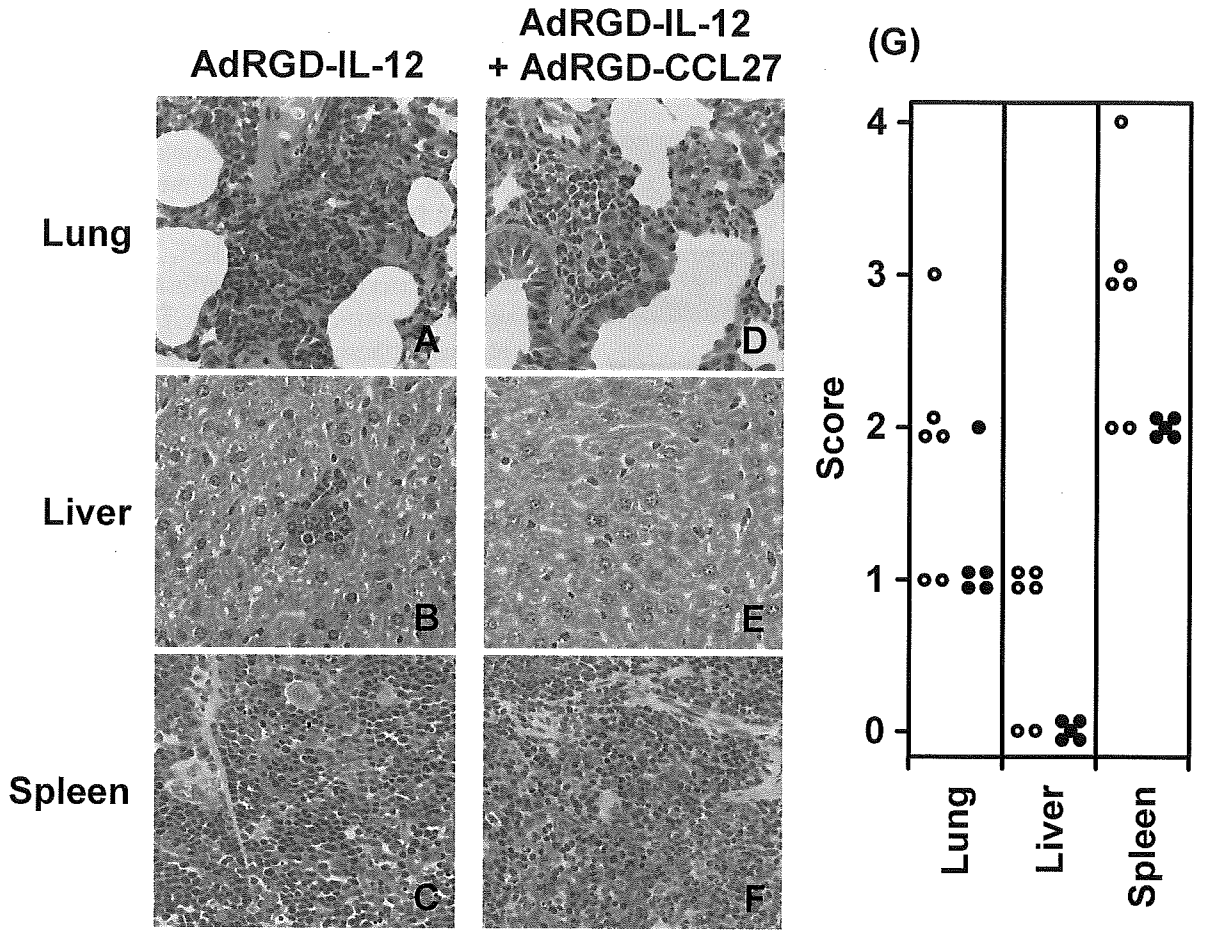

Fig.24 Histopathological examination of lung, liver, and spleen in Meth-A tumor-bearing mice treated with the AdRGD-IL12/AdRGD-CCL27 combination intratumoral injection.
BALB/c mice were intradermally inoculated with 2×10^6 Meth-A cells into the flanks. The tumors (7-9 mm in diameter) were injected with AdRGD-IL12 alone or the AdRGD-IL12 and AdRGD-CCL27 combination in a ratio of 9:1 at the same dose totaling 2×10^7 PFU. Three months later, lung (A and D), liver (B and E), and spleen (C and F) were harvested from mice in which the primary tumors were judged to have completely regressed, and then HE staining was performed using paraffin-embedded tissue sections. Original magnifications are ×300. (G): Histopathological changes (lymphocyte infiltration in lung and extramedullary hematopoiesis in liver and spleen) were scored as: 0, no; 1, rare; 2, mild; 3, moderate; 4, severe. (○); AdRGD-IL12 alone, (●); AdRGD-IL12 plus AdRGD-CCL27.

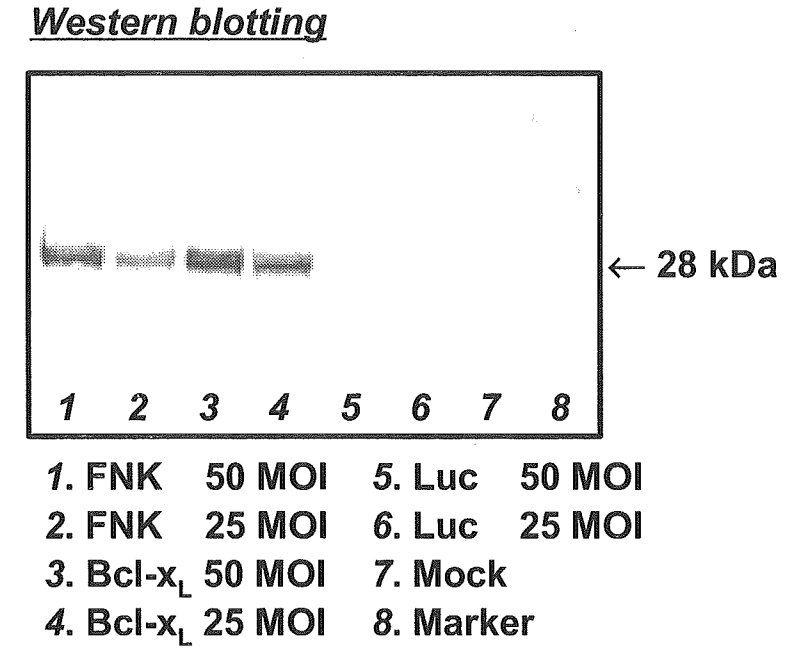

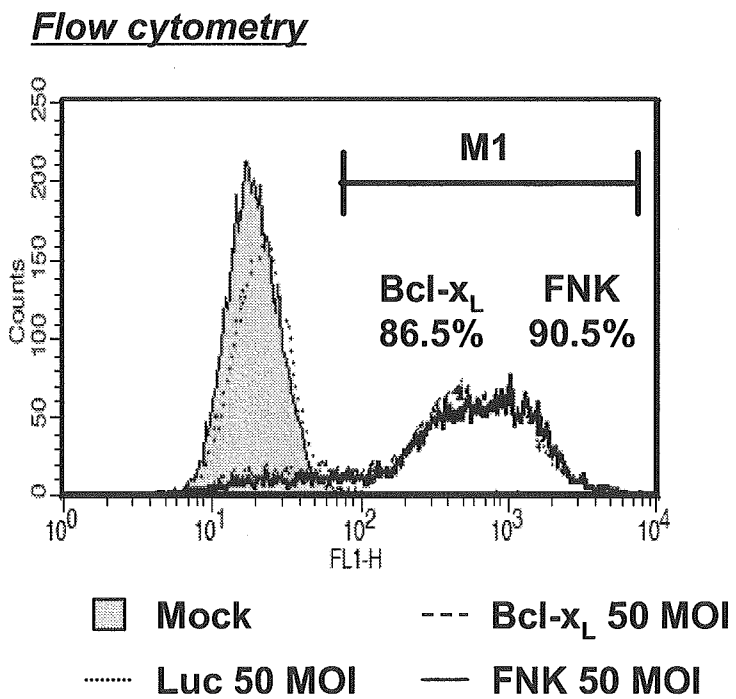

Fig.25 Gene expression analysis in A549 cells transfected with AdRGD-Bclx$_L$ or AdRGD-FNK. Human A549 cells were transfected with AdRGD-Bclx$_L$, AdRGD-FNK, or AdRGD-Luc at 50 MOI. After 48 h-culutivation, the expression of Bcl-x$_L$ or Bcl-xFNK proteins was assessed by both western blotting and flow cytometry analysis with an intracellular staining method. The % values in the lower panel express the percentage of M1-gated cells.

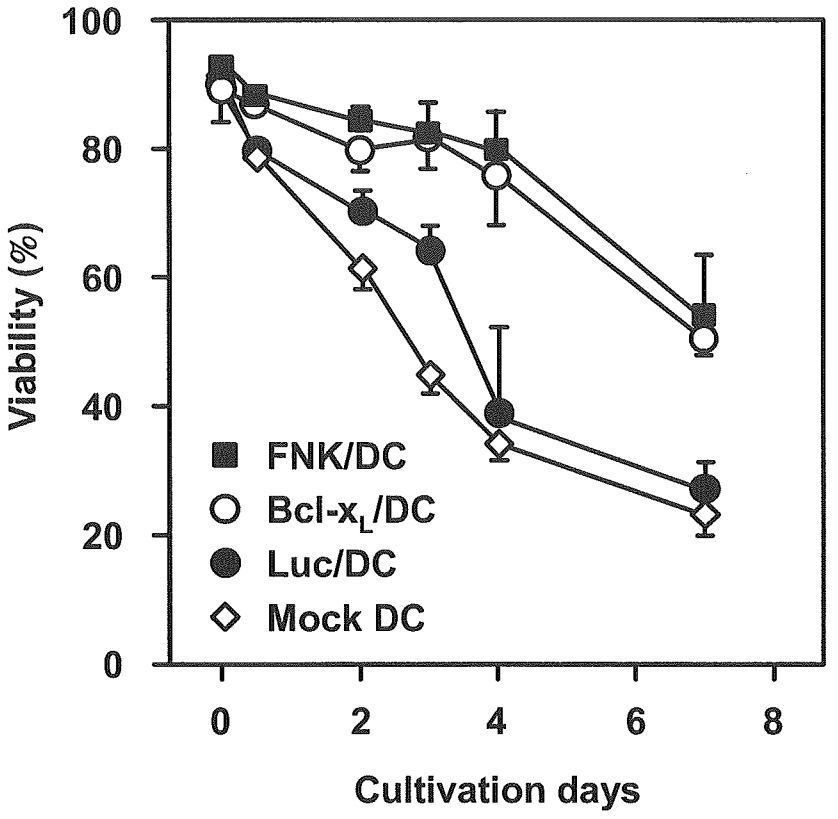

Fig.26 ***In vitro*** **viability of DCs transfected with AdRGD-Bclx$_L$ or AdRGD-FNK.**
FNK/DCs, Bcl-x$_L$/DCs, and Luc/DCs were prepared using corresponding vectors at 25 MOI, and then these transduced cells and mock DCs were cultured without cytokines and growth factors. The viability of DCs was assessed by propidium iodide staining at indicated cultivation days. Each point represents the means ± SE of triplicate cultures.

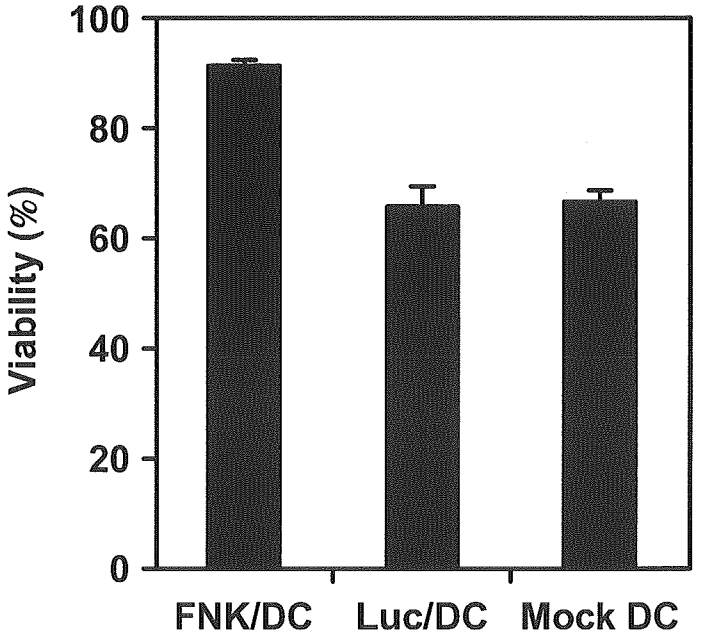

Fig.27 The resistance of FNK/DCs to apoptosis induced by staurosporine.
DCs were transfected with AdRGD-FNK or AdRGD-Luc at 50 MOI. After 48 h-cultivation, the transduced cells were cultured in the presence of 100 nM staurosporine for additional 24 h. The viability was assessed by MTT assay. Data are expressed as means ± SD of triplicate culture.

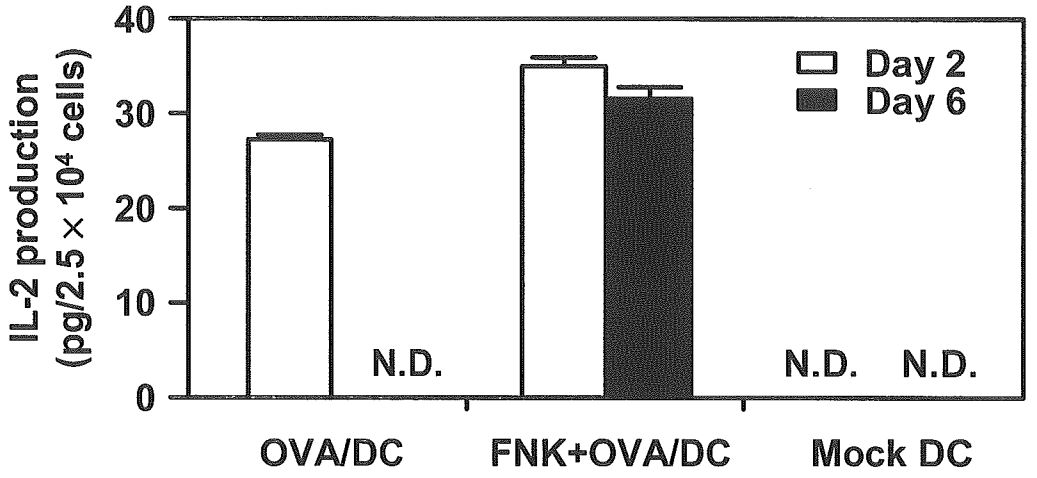

Fig.28 Duration of antigen presentation in FNK/DCs.
DCs were transfected with AdRGD-OVA alone (50 MOI) or the combination of AdRGD-OVA (50 MOI) and AdRGD-FNK (50 MOI) for 2 h. These transduced cells and mock DCs were cultured without cytokines and growth factors. On days 2 and 6, the levels of OVA-peptide presentation via MHC class I molecules on the transduced DCs were determined by bioassay using CD8-OVA1.3 cells. The data represents the means ± SD of three independent cultures. N.D.: IL-2 secreted from CD8-OVA1.3 cells was not detectable.

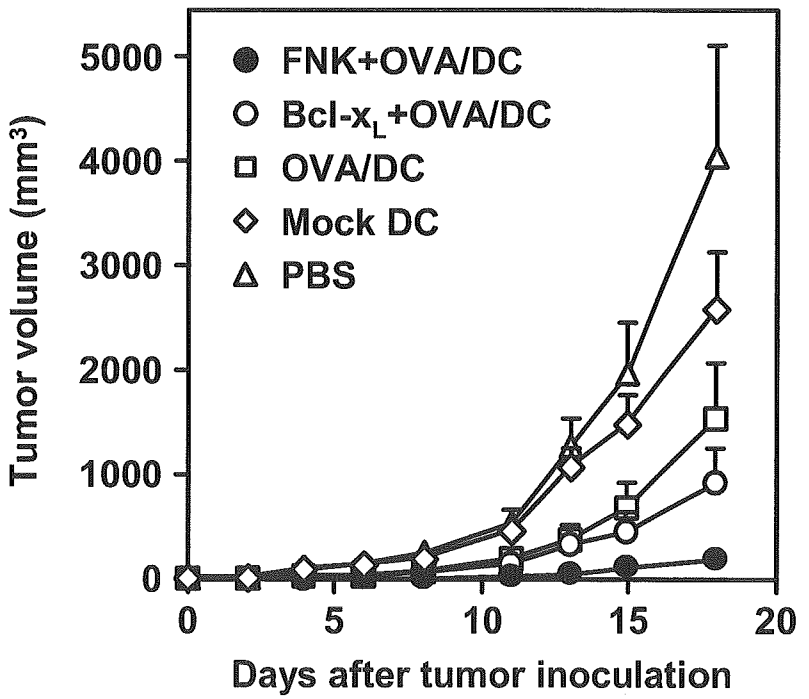

Fig.29 Vaccine efficacy of DCs co-transduced with OVA gene and either Bcl-x_L or Bcl-xFNK gene against E.G7-OVA challenge.
FNK+OVA/DCs, Bcl-x_L+OVA/DCs, and OVA/DCs were prepared using corresponding vectors at 25 MOI, and then cultures for 24 h. C57BL/6 mice were immunized by intradermal injection of transduced DCs into right flank at 5×10^4 cells. One week later, 10^6 E.G7-OVA cells were intradermaly inoculated into the left flank of these mice. The size of tumors was assessed using microcalipers three times per week. Each point represents the mean ± SE from 5-10mice.

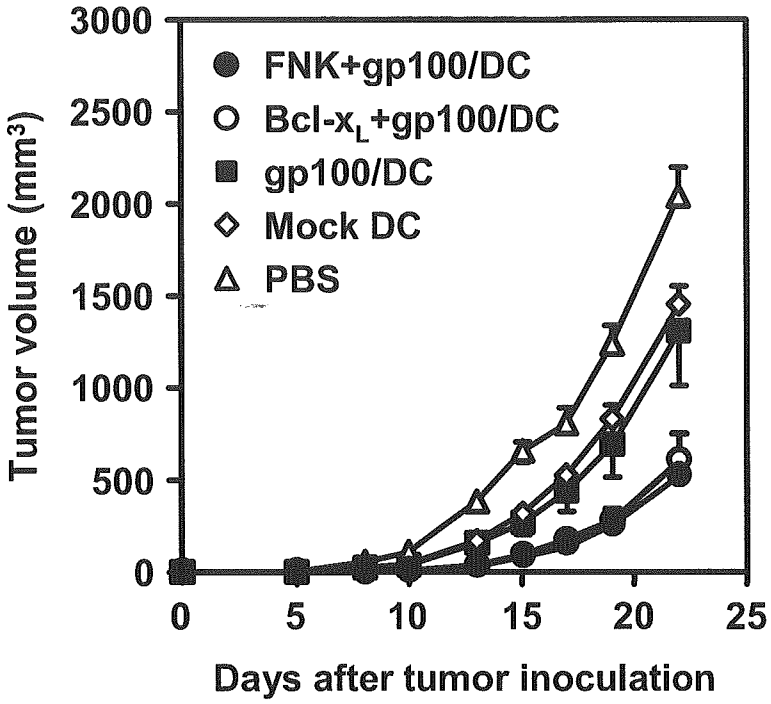

Fig.30 Vaccine efficacy of DCs co-transduced with gp100 gene and either Bcl-x_L or Bcl-xFNK gene against B16BL6 challenge.
FNK+gp100/DCs, Bcl-x_L+gp100/DCs, and gp100/DCs were prepared using corresponding vectors at 25 MOI, and then cultures for 24 h. C57BL/6 mice were immunized by intradermal injection of transduced DCs into right flank at 1.5×10^6 cells. One week later, 5×10^4 B16BL6 cells were intradermaly inoculated into the left flank of these mice. The size of tumors was assessed using microcalipers three times per week. Each point represents the mean ± SE from 5-10mice.

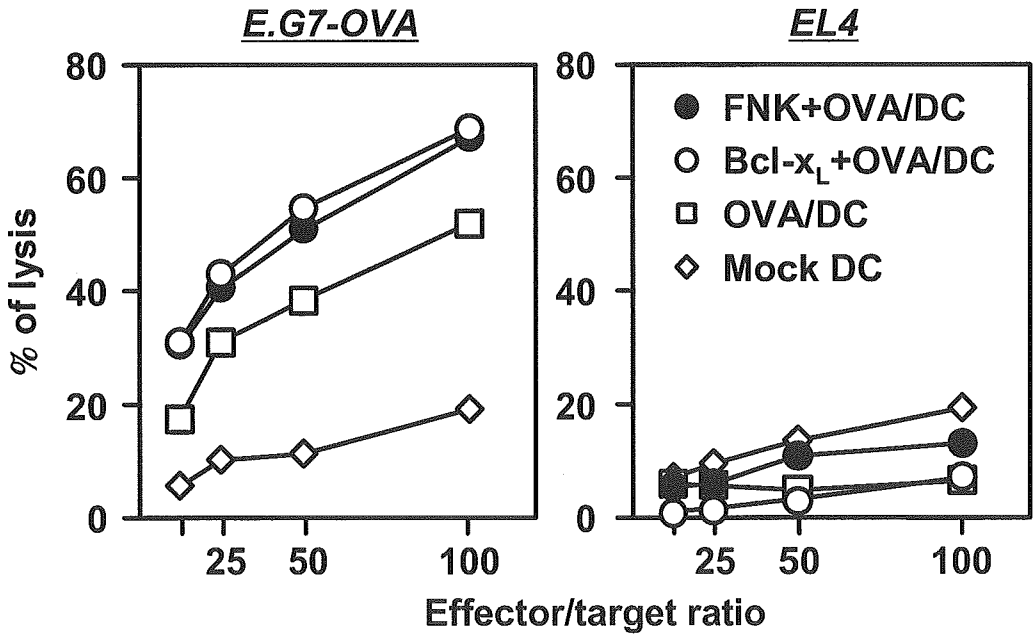

Fig.31 OVA-specific CTL response in mice immunized with DCs cotransduced with OVA gene and either Bcl-x_L or Bcl-xFNK gene.
FNK+OVA/DCs, Bcl-x_L+OVA/DCs, and OVA/DCs were prepared using corresponding vectors at 25 MOI, and then culture for 24 h. These transduced cells and mock DCs were vaccinated once intradermally into C57BL/6 mice at 2.5×10^4 cells. At 1 week after immunization, splenocytes were prepared from these mice, and were re-stimulated *in vitro* for 5 days with mitomycine C- inactivated E.G7-OVA cells. Cytolytic effects of re-stimulated splenocytes (effector cells) against E.G7-OVA or EL4 cells (target cells) were evaluated by ^{51}Cr-release assay.